Int. J. Electrochem. Sci., 10 **(2015)** 3726 - 3737

International Journal of
ELECTROCHEMICAL
SCIENCE
www.electrochemsci.org

Fabrication of a Nonenzymatic Glucose Sensor Based on Multi-Walled Carbon Nanotubes Decorated with Platinum and Silver Hybrid Composite

Kuo-Chiang Lin, Cheng-Yu Yang, Shen-Ming Chen[*]

Electroanalysis and Bioelectrochemistry Lab, Department of Chemical Engineering and Biotechnology, National Taipei University of Technology, No. 1, Section 3, Chung-Hsiao East Road, Taipei 106, Taiwan.
[*]E-mail: smchen78@ms15.hinet.net

Received: 5 Jan 2015 / *Accepted:* 22 February 2015 / *Published:* 23 March 2015

Novel platinum and silver decorated multi-walled carbon nanotubes (PtAg/MWCNTs) have been successfully prepared on electrode surface for nonenzymatic glucose detection. X-ray diffraction (XRD) and atomic force microscopy (AFM) analyses reveal that the Pt and Ag NPs were successfully deposited on the MWCNTs in this hybrid composite. In neutral condition, the electrode shows good activity towards glucose oxidation with low overpotential (-0.35 V vs. Ag/AgCl) and a current response that is 2.5–20 times greater than that obtained using Pt/MWCNTs/GCE and Ag/MWCNT/GCE. The optimised condition based on current response is found at pH 1. Voltammograms indicate a linear range of 1–25 mM with sensitivity of 115.8 μA mM^{-1} cm^{-2}. This electrode can effectively analyse glucose concentration in bovine serum albumin samples. It shows advantages with low overpotential, high sensitivity, good stability, and low cost.

Keywords: Glucose sensor, Platinum, Silver, Nanoparticles, Carbon nanotubes

1. INTRODUCTION

Glucose sensors can be classified as enzymatic sensors and nonenzymatic glucose sensors. Owing to the high selectivity and fast response of enzyme reaction, glucose oxidase has been widely used as amperometric biosensors [1–5]. However, due to the intrinsic feature of enzymes, the enzymatic biosensors always suffer from stability problems and can be easily affected by temperature, pH value, humidity, and toxic chemicals [6–8]. Therefore, the investigation of nonenzymatic glucose sensor which has the potential ability to become a cheap, stable, and sensitive enzyme-free sensor

toward glucose detection [9–11] is necessary and will provide important insight on these issues. To address these problems, many attempts have been made to construct nonenzymatic glucose sensor.

Nonenzymatic electro-oxidation of glucose could avoid the disadvantages of enzyme electrode [12]. The majority of nonenzymatic electrochemical glucose sensors mainly rely on the current response of glucose oxidation directly at the electrode surface [13]; thus, nonenzymatic glucose sensors have higher stability than enzymatic sensors. Therefore, more and more attempts have been made to construct nonenzymatic sensors for glucose detection in recent years [14–18].

The electrochemical nonenzymatic glucose sensors (such as alloys, noble metal platinum-based nanocomposites, metal oxides, etc.) have been widely reported [19]. Copper and nickel based catalysts are worth of developing and have been broadly used in the fabrication of nonenzymatic glucose sensors [20–27]. As is well known, large-scale commercial nonenzymatic glucose sensors are platinum-based materials. However, they are limited by their poor operational stability, low reserves, high cost, and low antitoxic ability. In order to enhance the stability, antitoxic ability and reduce the Pt usage, a lot of Pt-based binary catalysts in a general format of PtM (M = Ag, Co, Pb, Ni, etc.) have been studied [28–31], and most of them show good electrocatalytic property, non-toxicity, and long-term stability.

Different metals and metal oxides, such as Pt [32], Au [33], and Ni [34], and alloys containing Pt, Pb [35], Au, and Pd have been explored as catalysts of glucose sensors. Among these catalysts, Pt nanoparticles (NPs) are one of the most efficient for glucose oxidation because of their outstanding catalytic activity and anti-fouling property.

Since silver nanoparticles (AgNPs) have excellent electrical conductivity, they have been traditionally explored as catalysts in various reactions [36]. The immobilization of AgNPs onto electrode may lead to the large enhancement in the sensitivity of sensor [37].

Carbon nanomaterials, such as carbon nanotubes (CNTs) [38] and graphene [39], are commonly used to load catalysts for glucose sensor fabrication because of their unique physical and chemical properties.

In this work, electrocodeposition may be an effective way to prepare the Pt/Ag catalyst. Using electrocodeposition as preparation method, Pt/Ag/MWCNT is successfully prepared on glassy carbon electrode (GCE). When Pt/Ag/MWCNT/GCE is used as an enzyme-free glucose sensor, it exhibits excellent catalytic activity, selectivity, and high stability. Real sample analysis shows that Pt/Ag/MWCNT/GCE can be potentially used in detection of glucose in bovine serum albumin. This work is of great significance because it not only develops a simple and effective method to prepare Pt/Ag/MWCNT nanocomposites, but also the material may be used as nonenzymatic glucose biosensor.

2. EXPERIMENTAL

2.1. Reagents

Dihydrogen hexachloroplatinate(IV) (H_2PtCl_6), and multi-walled carbon nanotubes (MWCNTs) were purchased from Sigma-Aldrich (USA) and used as received. All other chemicals

(Merck) used were of analytical grade (99%). Double-distilled deionised water (> 18.1 MΩ cm^{-1}) was used to prepare all solutions. All other reagents were of analytical grade and used without further purification.

2.2. Apparatus and measurements

The PtAg/MWCNTs hybrid composite was characterised by atomic force microscopy (AFM) and X-ray diffraction (XRD). The electrochemical experiments were conducted using a CHI 1205a electrochemical workstation (CH Instruments, USA) with a conventional three-electrode setup using the PtAg/MWCNTs/GCE as the working electrode, an Ag/AgCl (3 M KCl) reference electrode, and a platinum wire counter electrode. A BAS (Bioanalytical Systems, Inc., USA) glassy carbon electrode (GCE) with a diameter of 0.3 cm was used for all electrochemical experiments. All potentials reported in this paper were referred to a Ag/AgCl electrode. The buffer solution was completely deaerated using a nitrogen gas atmosphere. The electrochemical cells were kept properly sealed to avoid interference with oxygen from the atmosphere. The composite was analysed by XRD, and its morphology was characterised by AFM using a tapping-mode scanning probe microscope (Being Nano-Instruments CSPM-4000, China). Indium tin oxide (ITO) was used as the substrate for various films in the AFM and XRD analyses.

2.3. Preparation of the PtAg/MWCNTs modified electrodes

GCE and ITO substrates were coated with different composites, including Pt, Ag, MWCNTs, PtAg, Pt/MWCNTs, Ag/MWCNTs, and PtAg/MWCNTs.

The Pt or Ag or PtAg electro-deposition was easily carried out in a sulphuric solution (pH 1.5) containing 1×10^{-2} M H_2PtCl_6 or/and 1.5×10^{-3} M $AgNO_3$ by consecutive cyclic voltammetry in the potential range of -0.5–1.0 V with a scan rate of 0.1 Vs^{-1} and 20 scan cycles. This method was used to prepare Pt, Ag, PtAg, Pt/MWCNTs, Ag/MWCNTs, and PtAg/MWCNTs modified electrodes.

Prior to the preparation of MWCNTs-modified electrodes, all MWCNTs were functionalised with carboxylic groups to confer good dispersion in the prepared solution [40]. This MWCNT solution was drop-casted on the electrode surface to form a MWCNTs-modified electrode. 10 μL of the MWCNT solution was used in this work to ensure coverage of the entire electrode surface. Next, the effluent from the effective surface area was carefully removed. The electrodes were cleaned and dried in an oven at 40 ºC. The MWCNTs-modified electrodes (MWCNTs/GCE and MWCNTs/ITO) were easily prepared using this method. Metal-MWCNTs films were successfully formed based on the preparation of related composites including Pt and Ag NPs can be sequentially deposited on MWCNTs.

All modified electrodes, namely, the Pt, Ag, PtAg, Pt/MWCNTs, Ag/MWCNTs, and PtAg/MWCNTs electrodes, were stored at room temperature before use.

3. RESULTS AND DISCUSSION

3.1. Characterisation of the PtAg/MWCNTs nanocomposite

A simple electrochemical synthesis of PtAg/MWCNTs hybrid composite was presented in this work. This hybrid composite can be easily prepared by the electrochemical reduction of H_2PtCl_6 and $AgNO_3$ using a MWCNTs-modified electrode with suitable potential control. Fig. 1 shows the voltammograms of Pt, Ag, and PtAg electrodeposition using a MWCNTs-modified electrode. Fig. 1A depicts the typical voltammogram of platinum electrodeposition with current increase at characteristic peaks.

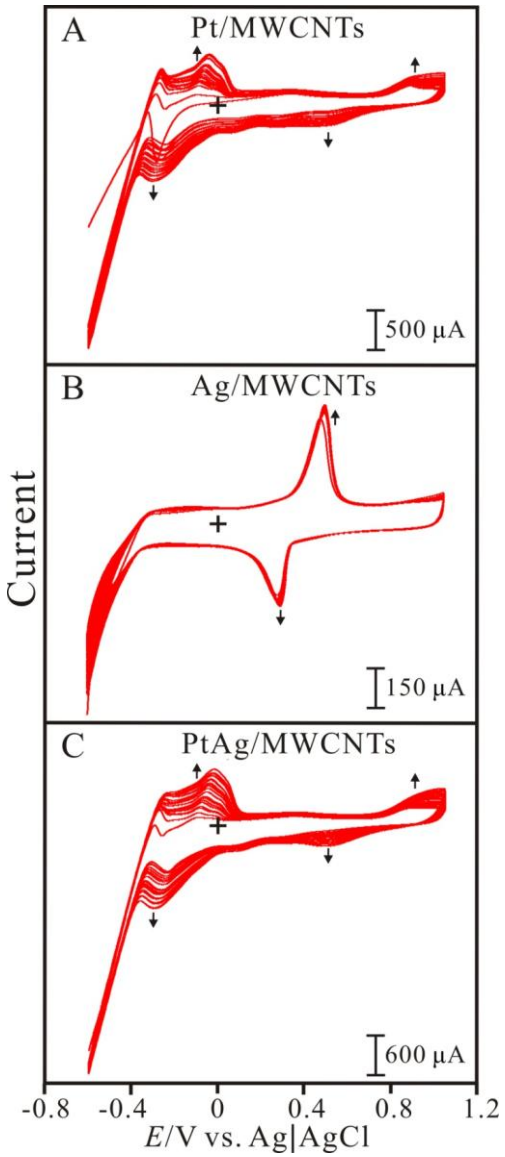

Figure 1. Consecutive cyclic voltammograms of MWCNTs/GCE examined in pH 1.5 sulphuric solution containing (A) 1×10^{-2} M H_2PtCl_6, (B) 1.5×10^{-3} M $AgNO_3$, and (C) 1×10^{-2} M H_2PtCl_6 + 1.5×10^{-3} M $AgNO_3$, respectively. Scan rate = 0.1 Vs^{-1}. 20 scan cycles.

Fig. 1B presents the voltammogram of Ag electrodeposition. It shows two characteristic peaks (E_{pa} = 0.45 V and E_{pc} = 0.25 V) involving Ag(I)/Ag(0) redox processes. Both anodic and cathodic peak currents increase with the increase in scan cycles, indicating the Ag electrodeposition can be well deposited on a MWCNTs-modified GCE. Fig. 1C shows the consecutive cyclic voltammograms of the PtAg electrocodeposition using a MWCNTs-modified GCE. It shows similar redox peaks related to Pt electrodeposition on a MWCNTs/GCE as shown in Fig. 1A. This phenomenon indicates they have similar electrochemical processes. Moreover, it shows about 100 μA current response higher than that of Pt/MWCNTs/GCE. It indicates the presence of Ag ions is helpful for Pt electrodeposition. However, no obvious Ag redox peaks found in the voltammogram. This result implies that the PtAg electrodeposition on a MWCNTs-modified GCE might be involving the Pt(shell)/Ag(core) deposition.

To verify the identity of the product, the composite was prepared on an ITO surface and examined by XRD. Fig. 2A shows the XRD patterns for (a) PtAg/MWCNTs/ITO, (b) MWCNTs/ITO, (c) PtAg/ITO, (d) Pt/ITO, and (e) Ag/ITO. These composites can be clearly identified using the standard patterns (Fig. 1B–D) for Pt, Ag, and ITO, respectively. When the MWCNTs was immobilised on ITO, it exhibited patterns (Fig. 1A(b)) almost identical to those of ITO. This phenomenon might indicate the MWCNTs is well dispersion and very thin on ITO surface. When PtAg/MWCNTs or PtAg or Pt was electrodeposited on the ITO (Fig. 1A(a) or (c) or (d)), five characteristic peaks were observed for Pt at 2θ = 40.04°, 46.54°, 67.86°, 81.51°, and 85.95°, corresponding to Miller indices (1 1 1), (2 0 0), (2 2 0), (3 1 1), and (2 2 2), respectively.

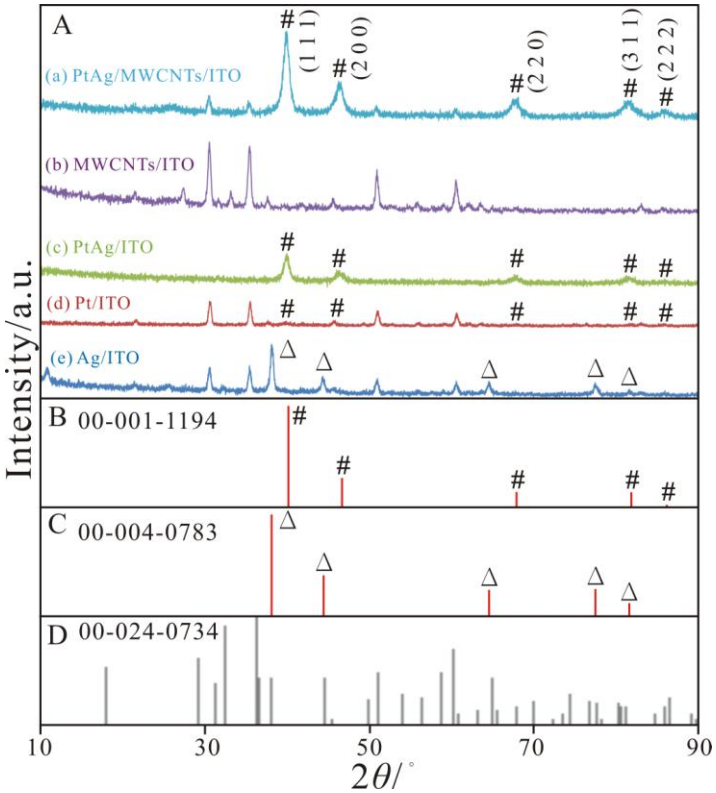

Figure 2. (A) XRD spectra of different modified ITO electrodes. Standard XRD patterns: (B) Pt, (C) Ag, and (D) ITO, respectively.

For Ag/ITO, it exhibits five characteristic peaks for Ag at 2θ = 38.12°, 44.28°, 64.43°, 77.48°, and 81.54°, corresponding to Miller indices (1 1 1), (2 0 0), (2 2 0), (3 1 1), and (2 2 2), respectively. One can know that both PtAg and PtAg/MWCNTs show no Ag patterns might prove that the Pt(shell)/Ag(core) formation in the electrodeposition of PtAg on both bare and MWCNTs-modified electrodes. One can conclude that the resultant particles are Pt(shell)/Ag(core) composites for the deposition on both bare and MWCNTs-modified electrodes.

The morphology of the different composites was studied by AFM. Fig. 3 shows the AFM images for (A) Pt/ITO, (B) Ag/ITO, (C) MWCNTs/ITO, and (D) PtAg/MWCNTs, respectively. The particle sizes for single and multi-composites were estimated and compared with those for the deposited material on the same scale. The average diameters were 37.2 nm, 90.1 nm, 46 nm, and 19 nm for Pt, Ag, MWCNTs, and PtAg/MWCNTs, respectively. Based on this comparison, both Pt and Ag particles are smaller when deposited on an MWCNT electrode. These findings indicate that MWCNTs may provide more suitable active sites for PtAg formation result in uniform particle distribution on electrode surface. Therefore, the PtAg/MWCNTs hybrid composites contain smaller particles than those of Pt, Ag, and MWCNTs.

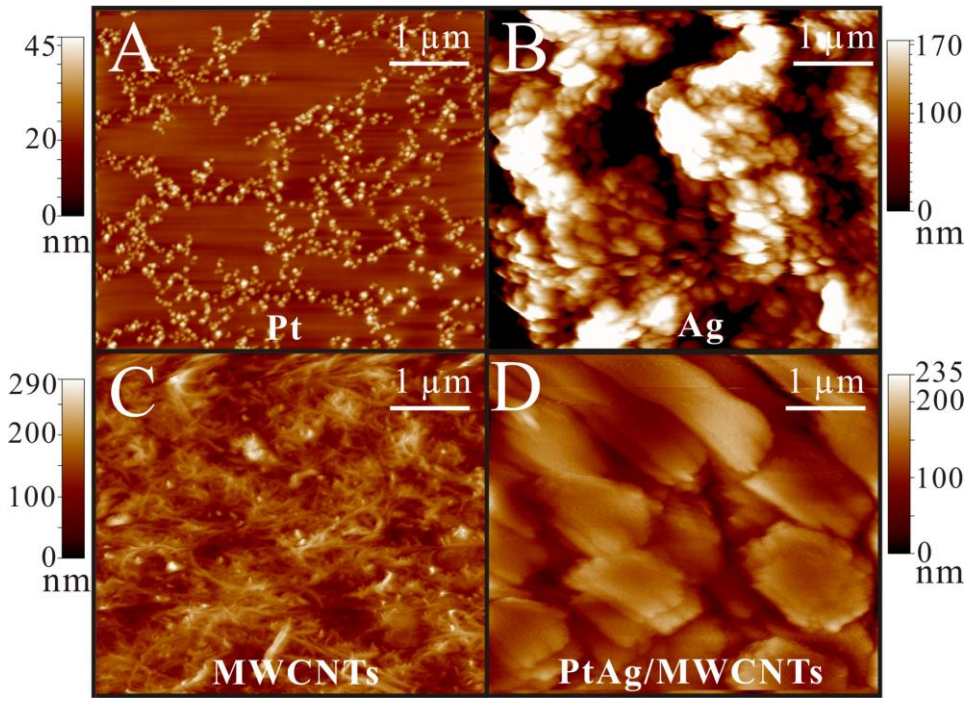

Figure 3. AFM images of (A) Pt, (B) Ag, (C) MWCNTs, and (D) PtAg/MWCNTs coated ITO electrodes.

3.2. Electrocatalysis of glucose at the PtAg/MWCNTs electrode

To explore the analytical applicability of the metal-MWCNT hybrid composites, the electrocatalytic activity of the different composite modified electrodes towards glucose oxidation was investigated by cyclic voltammetry.

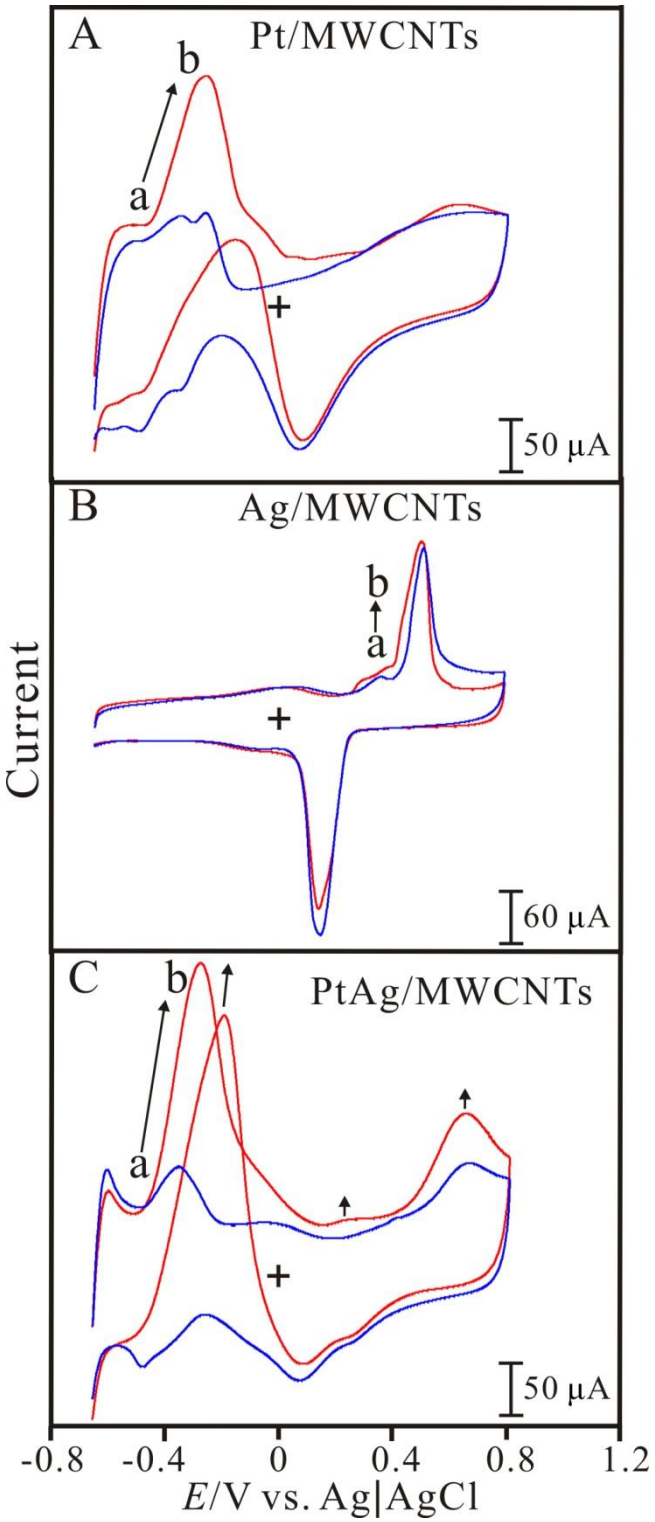

Figure 4. Cyclic voltammograms of (A) Pt/MWCNTs/GCE, (B) Ag/MWCNTs/GCE, (C) PtAg/MWCNTs/GCE examined in the (a) absence and (b) presence of 24 mM glucose (pH 7 PBS). Scan rate = 0.05 Vs^{-1}.

Fig. 4 shows the voltammograms of (A) Pt/MWCNTs, (B) Ag/MWCNTs, and (C) PtAg/MWCNTs modified electrodes examined in the absence/presence of 24 mM glucose (pH 7 PBS). As shown in Fig. 4A, the Pt/MWCNTs shows three obvious electrocatalytic oxidation peaks at -0.3 V,

-0.15 V, and +0.6 V, respectively. As shown in Fig. 4B, the Ag/MWCNTs shows two obvious electrocatalytic oxidation peaks at +0.3 V and +0.5 V, respectively. Particularly, the PtAg/MWCNTs shows four obvious electrocatalytic oxidation peaks at -0.35 V, -0.2 V, +0.2 V, and +0.6 V, which are similar to those of Pt/MWCNTs and Ag/MWCNTs. The electrocatalytic oxidation peaks are evaluated as shown in Table 1. The PtAg/MWCNTs shows a current response that is 1.4–26 times greater than that of the related modifiers. It also shows 2.5–20 times greater than that obtained using Pt/MWCNTs/GCE and Ag/MWCNT/GCE. One can conclude that the PtAg/MWCNTs almost maintain the electrocatalytic activities of Pt/MWCNTs and Ag/MWCNTs.

Table 1. Electrocatalytic oxidation peaks and net current for glucose oxidation using different modifiers in pH 7 PBS.

Modifiers	E_{pa} [a] /V	ΔI_{pa} [b]/μA
Pt	-0.32	51.3
	-0.05	57
	0.15	42
	0.65	42
Pt/MWCNTs	-0.30	141.6
	-0.15	61.7
	0.60	11.1
Ag	0.30	7.6
Ag/MWCNTs	0.30	10
	0.50	0.8
PtAg	-0.27	69.1
	-0.18	52.8
	0.20	8.4
	0.65	6.3
PtAg/MWCNTs(10:1.5)	-0.35	197
	-0.20	65.3
	0.20	17.6
	0.65	48.5

[a] The electrocatalytic oxidation peak estimated at the anodic peak which response oxidation current in the presence of 24 mM glucose.
[b] The net current estimated at the electrocatalytic peak in the absence/presence of 24 mM glucose.

Fig. 5 shows the voltammograms of PtAg/MWCNTs/GCE examined in pH 7 PBS with various glucose concentrations. The inset shows the linear correlation between current response and glucose concentration. It provides a linear concentration range of 1－25 mM with sensitivity of 115.8 μA mM^{-1} cm^{-2}. Fig. 6 shows the cyclic voltammograms of PtAg/MWCNTs/GCE examined at various pH values in the absence/presence of 1×10^{-3} M glucose. The anodic peak current (I_{pa}) increases obviously with increasing pH except of pH 1. The anodic current change (ΔI_{pa}) was the result estimated by the I_{pa}

value in the absence/presence of 1×10^{-3} M glucose. The ΔI_{pa} value also increases with increasing pH from pH 7 to 13. It indicates that the hybrid composite is better able to perform the electrocatalytic oxidation of glucose in the hydroxide-rich solution. Particularly, a high ΔI_{pa} value is found for pH 1 (inset of Fig. 6), suggesting this value as the optimised pH condition for glucose oxidation. The composite is further presenting in neutral condition due to its practical application for glucose testing.

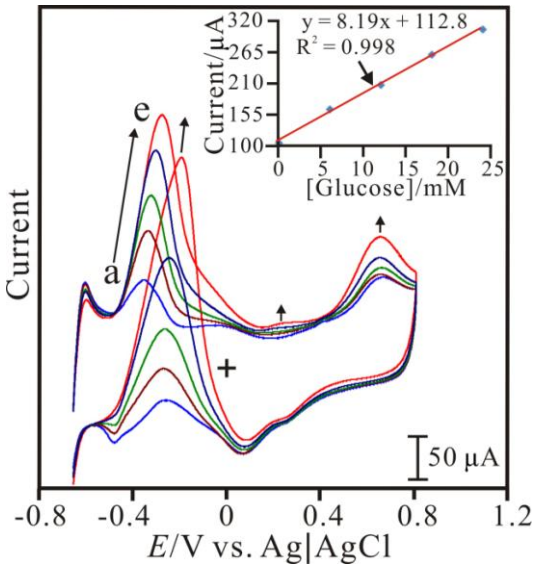

Figure 5. Cyclic voltammograms of PtAg/MWCNTs/GCE examined in pH 7 PBS containing [Glucose] = (a) 0, (b) 6 mM, (c) 12 mM, (d) 18 mM, and (e) 24 mM, respectively. Scan rate = 0.05 Vs^{-1}. Inset: the plot of the anodic peak current (I_{pa} measured at about -0.35 V) vs. glucose concentration.

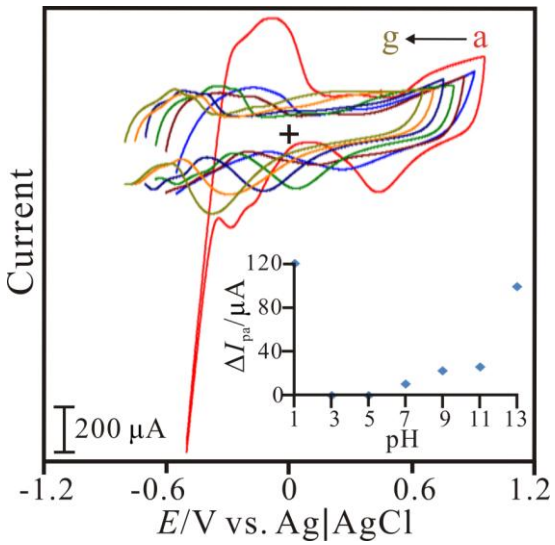

Figure 6. Cyclic voltammograms of PtAg/MWCNTs/GCE examined with (a) pH 1, (b) pH 3, (c) pH 5, (d) pH 7, (e) pH 9, (f) pH 11, and (g) pH 13, respectively. Scan rate = 0.05 Vs^{-1}. Inset: the plot of the contributed current of PtAg/MWCNTs/GCE estimated in the absence/presence of 1 mM glucose for different pH conditions.

3.3. Differential pulse voltammograms of PtAg/MWCNTs electrode to glucose

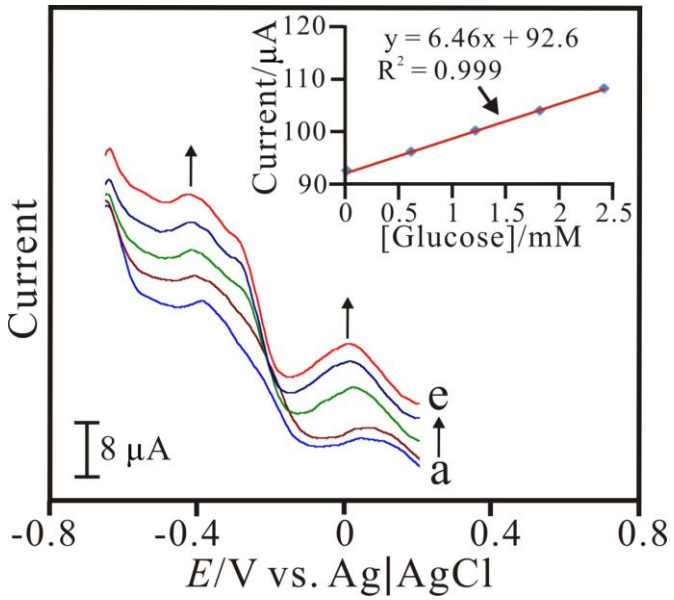

Figure 7. Differential pulse voltammograms of PtAg/MWCNTs/SPCE examined in pH 7 PBS containing [Glucose] = (a) 0, (b) 0.6 mM, (c) 1.2 mM, (d) 1.8 mM, and (e) 2.4 mM, respectively. Inset: the plot of the anodic peak current (measured at about -0.4 V) vs. glucose concentration.

Table 2. Performance of the PtAg/MWCNTs electrode compared with other modifiers for nonenzymatic glucose oxidation.

Modifiers	Applied potential (V vs. Ag/AgCl)	Sensitivity ($\mu A\ mM^{-1}\ cm^{-2}$)	Linear range (M)	Detection limit (μM)	Reference
Porous Au (Amperometry)	0.35	11.8	2×10^{-3}–1×10^{-2}	5	[41]
Mesoporous Pt (Amperometry)	0.4	9.6	0–1×10^{-2}	–	[42]
MWCNT (Amperometry)	0.2	4.4	2×10^{-6}–1.1×10^{-2}	1	[43]
Cu nanoparticles (Amperometry)	0.65	-	1×10^{-6}–5×10^{-3}	0.5	[44]
Pt nanotubes (Amperometry)	0.4	0.1	2×10^{-3}–1.4×10^{-2}	1	[45]
Pt–Pb/CNTs (Amperometry)	0.3	17.8	Up to 1.1×10^{-2}	1.8	[46]
PtAg/MWCNTs (DPV)	-0.4	91.4	1×10^{-3}–2.4×10^{-3}	600	This work

Fig. 7 shows the differential pulse voltammograms of the PtAg/MWCNTs electrode examined with several additions of 600 μM glucose in bovine serum albumin samples (pH 7 PBS). The anodic peak currents are increasing with the increase of glucose concentration. It shows three obvious anodic

peaks at about -0.4 V, -0.3 V, and 0 V, respectively. The calibration curve for the glucose sensor is shown in the inset of Fig. 7, which provides the regression equation, $I_{pa}(\mu A) = 6.46c_{glucose}(mM) + 92.6$, with correlation coefficient of $R^2 = 0.999$. The electrode has a linear concentration range of $1–2.4\times10^{-3}$ M with sensitivity of 91.4 μA mM^{-1} cm^{-2}. Based on the result, the PtAg/MWCNTs electrode is able to determine glucose in bovine serum albumin samples. As shown in Table 2, this sensor shows competitive performance especially for its low overpotential towards glucose oxidation.

4. CONCLUSIONS

We have successfully deposited Pt and Ag nanoparticles on the MWCNT modified electrode by cyclic voltammetry. The PtAg/MWCNTs electrode, a novel nonenzymatic glucose sensor, presents attractive features, such as low overpotential, simple synthesis, low cost, and test in neutral condition. The PtAg/MWCNTs modified screen printed electrode can be used for the analysis of glucose in bovine serum albumin samples. Based on the nonenzymatic glucose determination literature, it is competitive for the effective determination of glucose with simple method, low cost, and low overpotential.

ACKNOWLEDGMENTS
We acknowledge the Ministry of Science and Technology (Project No. 101-2113-M-027-001-MY3), Taiwan.

References

1. A. Riklin, E. Katz, I. Willner, A. Stocker, A.F. Buckmann, *Nature* 376 (1995) 672–675.
2. B.Z. Chi, Q. Zeng, J.H. Jiang, G.L. Shen, R.Q. Yu, *Sens. Actuators B* 140 (2009) 591–596.
3. H. Tang, F. Yan, Q. Tai, H.L.W. Chan, *Biosens. Bioelectron.* 25 (2010) 1646–1651.
4. J. Shi, H.Y. Zhang, A. Snyder, M.X. Wang, J. Xie, D.M. Porterfield, L.A. Stanciu, *Biosens. Bioelectron.* 38 (2012) 314–320.
5. J. Shi, T.G. Cha, J.C. Claussen, A.R. Diggs, J.H. Choi, D.M. Porterfield, *Analyst* 136 (2011) 4916–4924.
6. M.D. Gouda, S.A. Singh, A.G.A. Rao, M.S. Thakur, N.G. Karanth, *J. Biol. Chem.* 278 (2003) 24324–24333.
7. Y. Liu, M.K. Wang, F. Zhao, Z. Xu, S.J. Dong, *Biosens. Bioelectron.* 21 (2005) 984–988.
8. Z.J. Wang, X.Z. Zhou, J. Zhang, F. Boey, H. Zhang, *J. Phys. Chem. C.* 113 (2009) 14071–14075.
9. B. Singh, F. Laffir, T. McCormac, E. Dempsey, *Sens. Actuators B* 150 (2010) 80–92.
10. J. Ryu, K. Kim, H.S. Kim, H.T. Hahn, D. Lashmore, *Biosens. Bioelectron.* 26 (2010) 602–607.
11. L. Zhang, H. Li, Y. Ni, J. Li, K. Liao, G. Zhao, *Electrochem. Commun.* 11 (2009) 812–815.
12. Y. Sun, H. Buck, T.E. Mallouk, *Anal. Chem.* 73 (2001) 1599–1604.
13. C.C. Mayorga-Martinez, M. Guix, R.E. Madrid, A. Merkoçi, *Chem. Commun.* 48 (2012) 1686–1688.
14. J. Zhao, L.M. Wei, C.H. Peng, Y.J. Su, Z. Yang, L.Y. Zhang, H. Wei, Y.F. Zhang, *Biosens. Bioelectron.* 47 (2013) 86–91.
15. G.M. Wang, X.H. Lu, T. Zhai, Y.C. Ling, H.Y. Wang, Y.X. Tong, Y. Li, *Nanoscale* 4 (2012) 3123–3217.

16. M.R. Guascito, D. Chirizzi, C. Malitesta, M. Siciliano, T. Siciliano, A. Tepore, *Electrochem. Commun.* 22 (2012) 45–48.
17. J. Yang, W.D. Zhang, S. Gunasekaran, *Biosens. Bioelectron.* 26 (2010) 279–284.
18. M.M. Liu, R. Liu, W. Chen, *Biosens. Bioelectron.* 45 (2013) 206–212.
19. S. Park, H. Boo, T. Chung, *Anal. Chim. Acta* 556 (2006) 46–57.
20. I. Yeo, D. Johnson, *J. Electroanal. Chem.* 484 (2000) 157–163.
21. N. Quoc Dung, D. Patil, H. Jung, D. Kim, *Biosens. Bioelectron.* 42(2013) 280–286.
22. F. Meng, W. Shi, Y. Sun, X. Zhu, G. Wu, C. Ruan, X. Liu, D. Ge, *Biosens. Bioelectron.* 42 (2013) 141–147.
23. M. Liu, R. Liu, W. Chen, *Biosens. Bioelectron.* 45 (2013) 206–212.
24. S. Meher, G. Rao, *Nanoscale* 5 (2013) 2089–2099.
25. X. Li, J. Yu, F. Liu, H. He, M. Zhou, N. Mao, P. Xiao, Y. Zhang, *Sens. Actuators B* 181 (2013) 501–508.
26. Y. Hu, Q. Shao, P. Wu, H. Zhang, C. Cai, *Electrochem. Commun.* 18 (2012) 96–99.
27. L.X. Ding, A.L. Wang, G.R. Li, Z.Q. Liu, W.X. Zhao, C.Y. Su, Y.X. Tong, *J. Am. Chem. Soc.* 134 (2012) 5730–5733.
28. C. Xu, Y. Liu, F. Su, A. Liu, H. Qiu, *Biosens. Bioelectron.* 27 (2011) 160–166.
29. F. Xiao, F. Zhao, D. Mei, Z. Mo, B. Zeng, *Biosens. Bioelectron.* 24(2009) 3481–3486.
30. X. Che, R. Yuan, Y. Chai, J. Li, Z. Song, W. Li, X. Zhong, *Colloids Surf. B* 84 (2011) 454–461.
31. J. Wang, D. Thomas, A. Chen, *Anal. Chem.* 80 (2008) 997–1004.
32. S. Park, R.A. Jeong, H. Boo, J. Park, H.C. Kim, T.D. Chung, *Biosens. Bioelectron.* 31 (2012) 284–291.
33. M. Pasta, F. La Mantia, Y. Cui, *Electrochim. Acta* 55 (2010) 5561–5568.
34. C.X. Wang, L.W. Yin, L.Y. Zhang, R. Gao, *J. Phys. Chem. C* 114 (2010) 4408–4418.
35. J.P. Wang, D.F. Thomas, A.C. Chen, *Anal. Chem.* 80 (2008) 997–1004.
36. X.L. Zhu, X. Gan, J. Wang, T. Chen, G.X. Li, *J. Mol. Catal. A: Chem.* 239 (2005) 201–204.
37. B. Zheng, G. Liu, A. Yao, Y. Xiao, J. Du, Y. Guo, D. Xiao, Q. Hu, M.M.F. Choi, *Sens. Actuators B* 195 (2014) 431–438.
38. B. Wu, Y. Kuang, X. Zhang, J. Chen, *Nano Today* 6 (2011) 75–90.
39. J.C. Claussen, A. Kumar, D.B. Jaroch, M.H. Khawaja, A.B. Hibbard, D.M. Porter-field, T.S. Fisher, *Adv. Funct. Mater.* 22 (2012) 3399–3405.
40. K.C. Lin, T.H. Tsai, S.M. Chen, *Biosens. Bioelectron.* 26 (2010) 608–614.
41. Y. Li, Y.Y. Song, C. Yang, X.H. Xia, *Electrochem. Commun.* 9 (2007) 981–988.
42. S. Park, T.D. Chung, H.C. Kim, *Anal. Chem.* 75 (2003) 3046–3049.
43. J.S. Ye, Y. Wen, W.D. Zhang, L.M. Gan, G.Q. Xu, F.S. Sheu, *Electrochem. Commun.* 6 (2004) 66–70.
44. Q. Xu, Y. Zhao, J.Z. Xu, J.J. Zhu, *Sens. Actuat. B* 114 (2006) 379–386.
45. J.H. Yuan, K. Wang, X.H. Xia, *Adv. Funct. Mater.* 15 (2005) 803–809.
46. H.F. Cui, J.S. Ye, W.D. Zhang, C.M. Li, J.H.T. Luong, F.S. Sheu, *Anal. Chim. Acta* 594 (2007) 175–183.